

Electronic Supplementary Information for

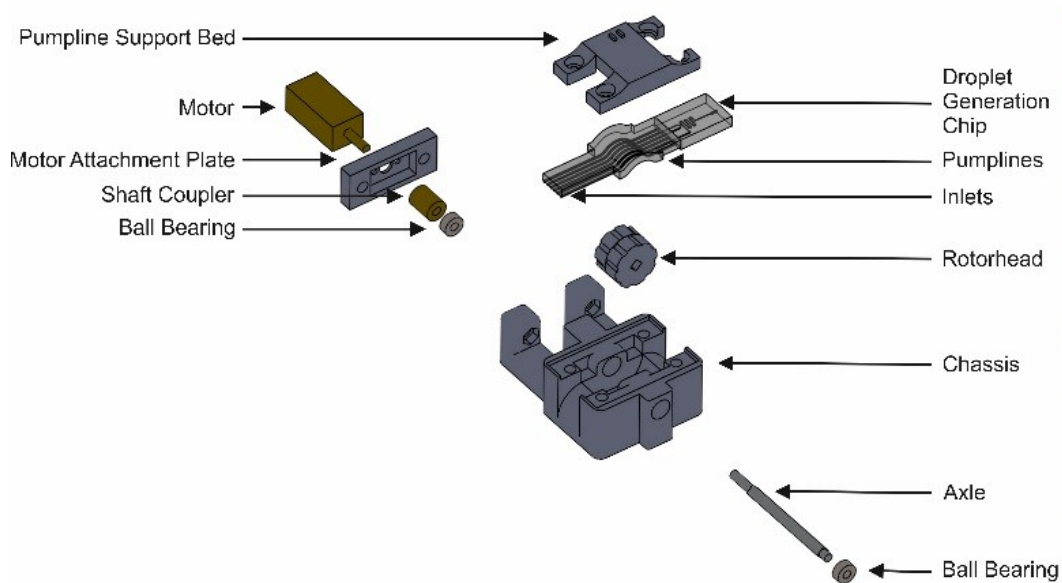
Phased peristaltic micropumping for continuous sampling and hardcoded droplet generation

Adrian M. Nightingale^{a,b}, Gareth W. H. Evans^{a,b}, Peixiang Xu^a, Byung Jae Kim^a, Sammer-ul Hassan^{a,b} and Xize Niu^{a,b,†}

^aFaculty of Engineering and the Environment, University of Southampton, Southampton, U.K. SO17 1BJ.

^bInstitute for Life Sciences, University of Southampton, Southampton, U.K. SO17 1BJ.

† Email: x.niu@soton.ac.uk



a)

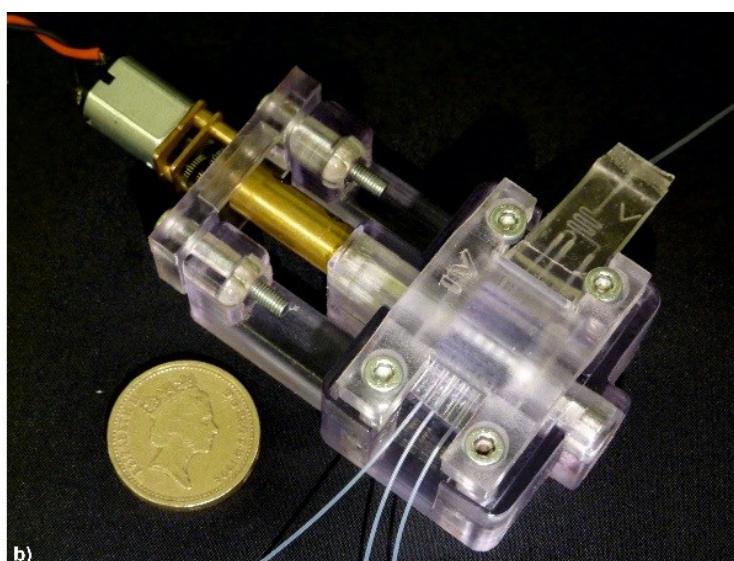


Figure S1: Schematic of peristaltic micropump b) Exploded view of the peristaltic micropump key components c) Photo of peristaltic micropump with a one pound coin (22.5 mm diameter) for scale.

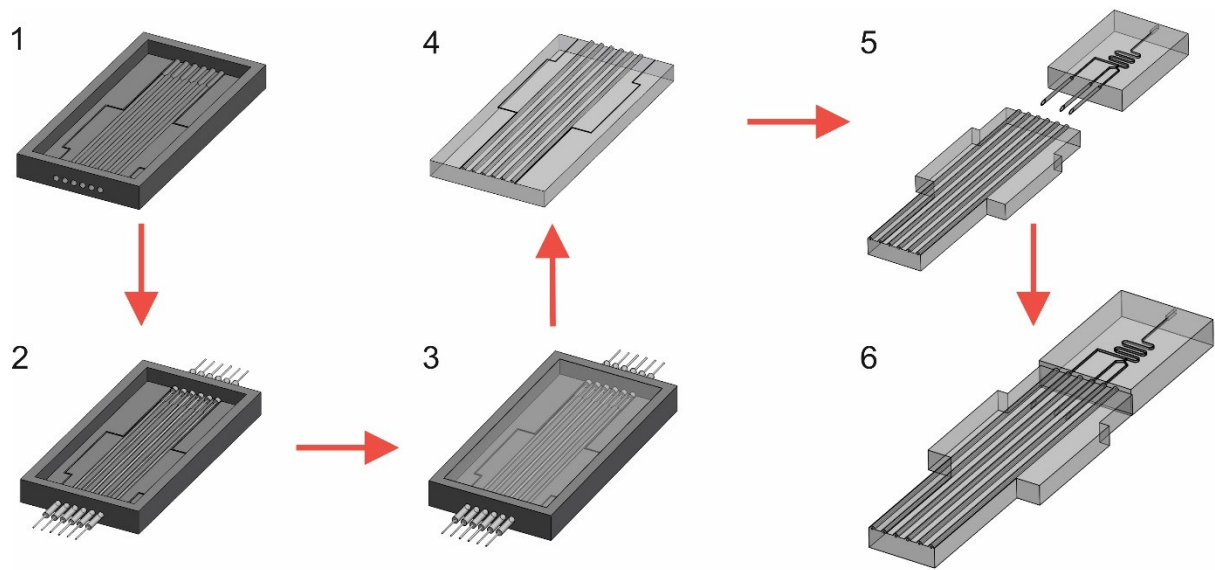


Figure S2: Manufacture of the monolithic microfluidic chip. 1) 3D printed mould. 2) Insertion of the fibre optics that template the channels. 3) PDMS is poured into the mould and fully cured at 70 °C. 4) Chip is removed from the mould and the fibre optics carefully removed. 5) Chip is cut to fit the pumpline support bed. 6) Pump chip is bonded to a droplet generation chip (produced by standard multilayer PDMS casting procedures¹) using short (~4 mm) 0.4 mm ID PTFE tubing connectors, and making the join permanent by an external coating of PDMS.

Droplet generation with higher viscosity aqueous phase

Having shown the droplet generation to be robust to changes in total flow rate (as described in the main text) we tested the effect of viscosity change, since microfluidic systems are often applied to the manipulation and analysis of viscous biological media². Solutions of different viscosity were made by dissolving sucrose in water at concentrations between 0 and 60 % by mass. These were then successively flowed through the pump and droplet generation chip, using a rotorhead with 8 features and a spacing of 1.94 mm and keeping the motor speed constant at 0.4 Hz. The droplets exited the chip into PTFE tubing (inner diameter 0.32 mm) where they were imaged using a USB microscope and the subsequent video analysed. Fig. S3 shows the obtained droplet sizes as a function of the sucrose loading (top) and corresponding viscosity (bottom, obtained from reference values³). The figure also shows reference viscosities of common biological fluids: blood serum, plasma, and whole blood at shear rates between 1 and 100 s⁻¹ – showing the viscosities tested were representative of typical biological media. Importantly, the mean droplet size was invariant with viscosity, again consistent with the proposed method of droplet generation and showing how this droplet generation technique is suitable for applications where biological fluids are sampled or processed. The ability of the pump to operate against an applied pressure was also tested by continuously pumping into a sealed container fitted with a pressure sensor (MPX4250A, RS, UK). The pump successfully operated above the pressure sensor's maximum of 1.6 bar.

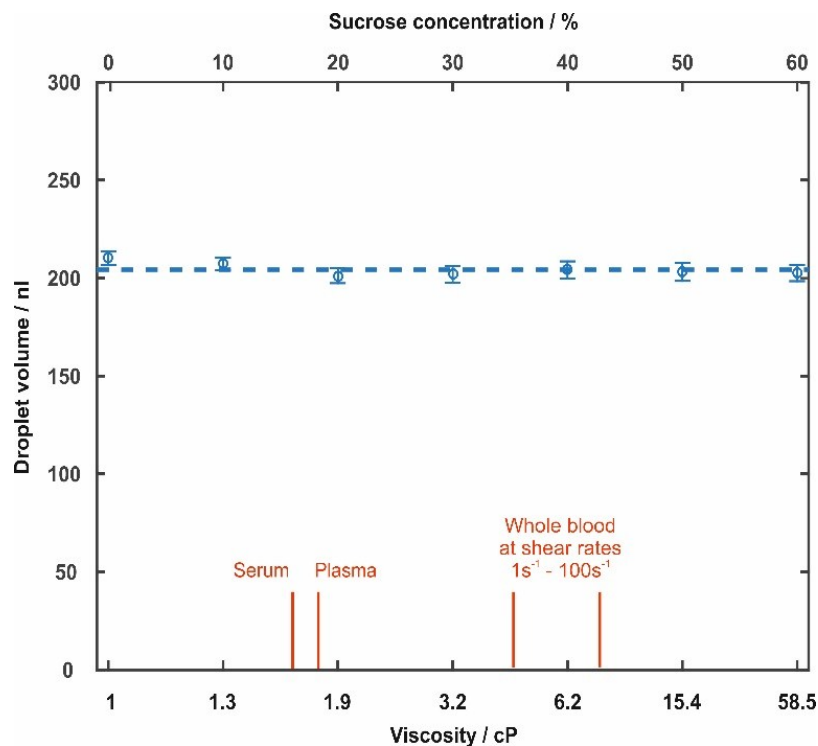


Figure S3: Droplet volume is constant with respect to viscosity for varying concentrations (by weight) of sucrose solution droplets (with viscosities encompassing a range of typical biological media viscosities, as indicated). Error bars represent the standard deviation of droplet volume.

Absorption flow cell for reaction kinetics measurement

To measure the reaction rates of an enzymatic glucose assay within droplets (as described in the main text) we used a flow cell composed of a series of concatenated absorption cells, each consisting of an LED, photodiode, and 3D printed support which positioned PTFE tubing (containing the droplet flow) in the light path. Each absorption cell measured at increasingly further distances downstream of the droplet generation chip. Thus with knowledge of the droplet velocity we could convert the distance to a residence time and monitor the change in droplet absorbance over time. The flow cell design has been described in detail in a previous report⁴ and is also shown below in Fig. S4.

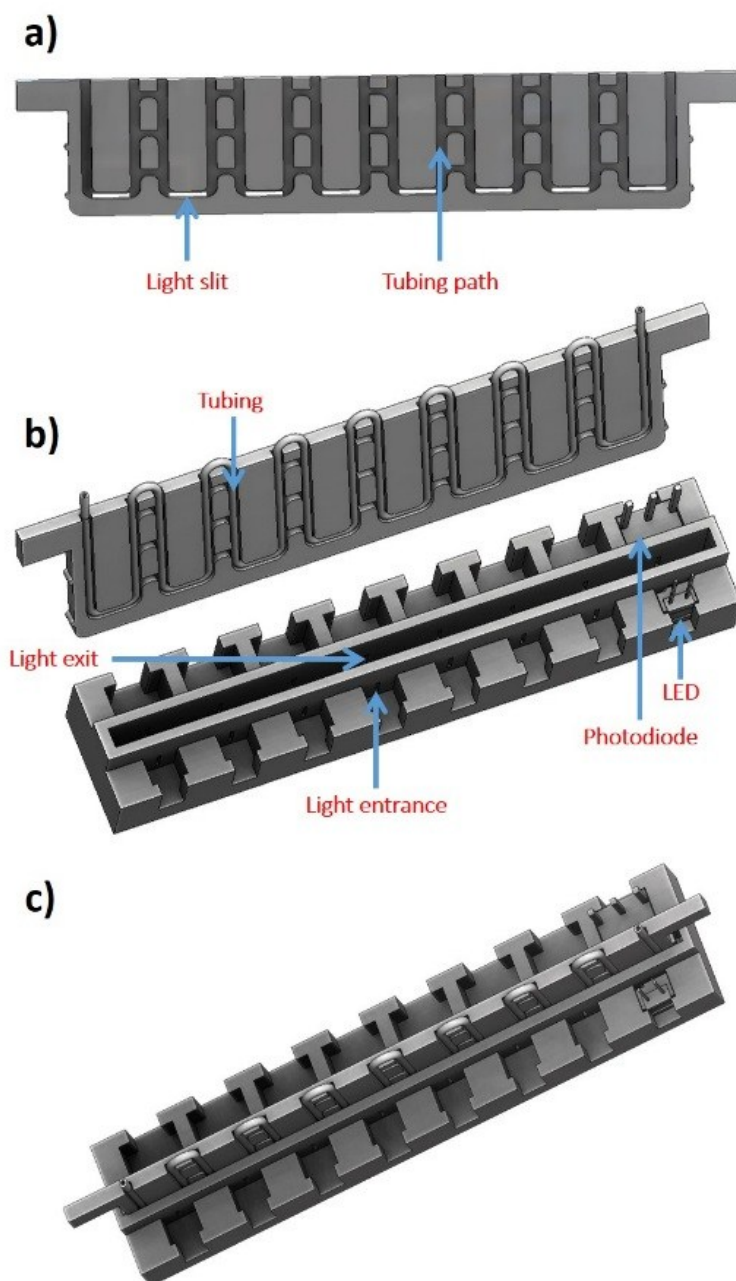


Figure S4: Schematics illustrating the 3D-printed multi-detector absorption flow cell used for inline reaction rate measurement. a) Cartridge into which the PTFE tubing carrying the droplet flow is inserted. b) The cartridge slots into a holder which contains an array of LEDs and photodiodes (only one LED and photodiode are shown in this image for clarity). Once inserted, light travels from each LED through a light entrance, through the tubing and a light slit in the cartridge, then through the light exit to the corresponding photodiode. c) The cartridge fully inserted within the holder. Full details of the flow cell fabrication and operation can be found in the previous report by Hassan et al.⁴.

Fig. S5 shows absorption results obtained using the flow cell for a single sequence of droplets of varying glucose concentration (1.18 – 5.44 mM). In each case, the absorption increases as it passes through the flow cell, with increased glucose concentrations giving more pronounced increases.

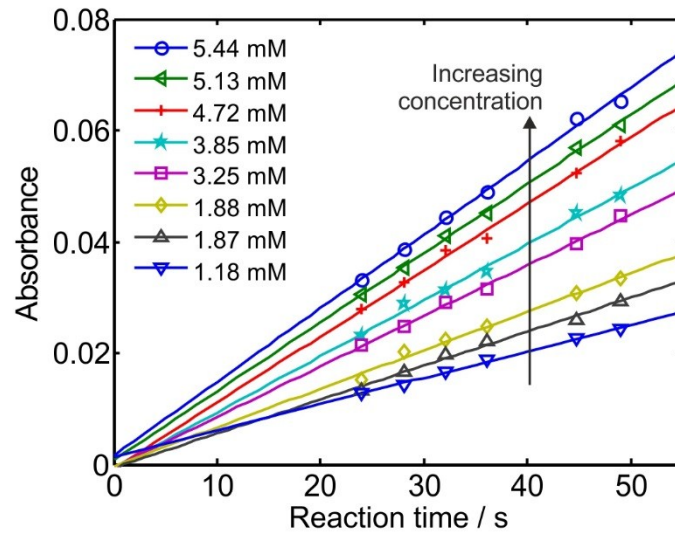


Figure S5: Absorbance over time for droplets within a single dilution sequence of varying glucose concentration. Each set of data is fitted with a line where the gradient corresponds to the reaction rate.

Rotorhead design

Basic dimensions

For all the work described here we used a rotorhead with the same basic dimensions – an outer diameter of 16.250 mm with troughs of depth 0.625 mm and curved shoulders of radius 0.625 mm (see Fig. S6a). This geometry was found to be a good fit to the pumpchip and its supporting bed. We have chosen to define the size of each feature by the distance, s (spacing) and angle, θ between the bottom of one shoulder to the bottom of the next as shown in Fig. S6a. While the spacing is a useful parameter for discussing the method of pumping and droplet generation (and was used exclusively in the main text), θ is a more useful quantity when calculating the dimensions of the rotorhead.

Feature design rules

The feature spacing can be varied as required providing the following design rules are adhered to:

- 1) The topography associated with a single pumpline must have an integral number of features.
- 2) Aqueous and oil features must be antiphased and the troughs must not overlap, as shown in Fig. S6b (See also the 3D models in Fig. 2e and the flattened topography shown in Fig. 6).
- 3) The aqueous and oil lines should have the same number of features.

Additionally we would recommend that:

- 4) The spacing not exceed 2.7 mm. Beyond this we found that the curvature of the rotorhead resulted in the centre of the trough contacting the pumpline and thus reducing the pumped volume.
- 5) The feature shoulder geometry remain constant (dimensions given above).

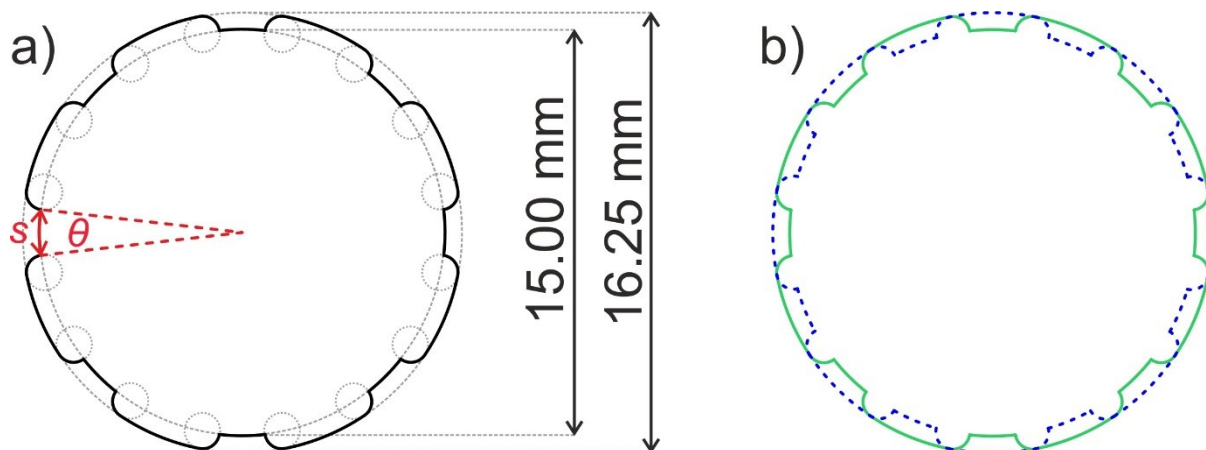


Figure S6: a) Schematic showing the basic geometry of a typical rotorhead in cross section. b) Schematic showing how the relative geometry of the oil (green solid line) and aqueous (blue dashed line) topography should have no overlap of the feature troughs. This ensures the two phases are pumped independently.

References

1. McDonald, J.C. & Whitesides, G.M. Poly(dimethylsiloxane) as a Material for Fabricating Microfluidic Devices. *Accounts of Chemical Research* **35**, 491-499 (2002).
2. Sackmann, E.K., Fulton, A.L. & Beebe, D.J. The present and future role of microfluidics in biomedical research. *Nature* **507**, 181-189 (2014).
3. Swindells, J.F., C.F., S., R.C., H. & P.E., G. Viscosities of Sucrose Solutions at various Temperatures Tables of Recalculated Values. *United States Department of Commerce National Bureau of Standards* (1958).
4. Hassan, S., Nightingale, A.M. & Niu, X. Continuous measurement of enzymatic kinetics in droplet flow for point-of-care monitoring. *Analyst* **141**, 3266-3273 (2016).